ADV MATH SCI JOURNAL
Advances in Mathematics: Scientific Journal **11** (2022), no.5, 469–497
ISSN: 1857-8365 (printed); 1857-8438 (electronic)
https://doi.org/10.37418/amsj.11.5.4

MODELISATION AND NUMERICAL SIMULATION OF SALT GRADIENT SOLAR POND: THE ALTERNATING DIRECTION IMPLICIT METHOD

Abdelli Ammar, Hocine Sissaoui, Messaoud Kermiche, and Bahi Oussama[1]

ABSTRACT. Solar energy as free and abundant energy is considered among the renewable energy that can replace disappearing fossil fuels. Many solar power systems can be used to capture this energy, but the majority does not have the ability to store this energy in different weather and time conditions. Therefore, salinity gradient solar ponds used in the present work can overcome this issue by simultaneously capturing and storing solar energy. A solar pond is being built at Annaba. In this present work we consider two identical solar ponds subjected to the same solar radiations during a period of 28 days, and exposed to the same climatic conditions, initial and at the limits. in the first pond, nanoparticles of conductive metal, namely copper, are injected with a concentration of 0.09%, while the second pond does not contain any nanoparticles. a comparative study was carried out on the temperature profile in the two solar ponds mentioned above to see the influence of nanoparticles on the thermal performance of the solar pond. The mathematical model adopted in this work is based on the equation of heat conduction in two dimensions with an external source of energy to the system. The method of finite differences with ADI scheme was used to determine the temperature distribution in two different directions according to the horizontal axis ox and to the vertical axis OZ representing the depth. An average temperature and insolation values for the last ten years were obtained using the data provided by Annaba saline station. Finally, a comprehensive study was carried out in order to highlight the convergence, consistency and stability properties of the discrete model representing the solar pond.

[1]*corresponding author*
2020 *Mathematics Subject Classification.* 00A72.
Key words and phrases. Solar pond, temperature distribution, filling time, ADI scheme, convergence, consistency and stability.
Submitted: 07.05.2022; *Accepted:* 20.05.2022; *Published:* 26.05.2022.

1. INTRODUCATION

The solar pond is a device that consists of capturing and storing solar energy using a salinity gradient. Its construction is simple and it is not expensive in economic terms, it requires no battery to store energy and it is well suited to rural and sunny areas. it does not represent any source of fossil fuel pollution with their associated pollution problems has led many scientists to conduct studies and investigations on this subject. it does not represent any source of pollution which led many researchers to conduct studies and investigations on this subject. The replacement of non-renewable fossil energy is a major challenge for humanity in the next years to come, due to the release of CO_2 which causes global warming. As a result, it is now essential to replace this energy with other renewable and clean sources. In this context, solar energy by its abundance (average of $800W/m2$) and as free of cost energy is potentially interesting. Several works have shown that it is possible to exploit this light energy by transforming it into different forms: electrical (photovoltaic), thermal (generation of vapors and others), chemical, etc. However, despite this abundance and availability, solar energy has not been able to replace fossil energy because, mainly, the high cost of storage. The salinity gradient solar pond can be a good alternative for the collection and especially the storage for a relatively long period of solar energy in thermal form. This pond is the cheapest mean energy storage known to date. The idea of the solar pond appears in 1902 when Kalecsinsky was observed in Transylvania than in natural saline lakes, the temperature at a depth of $1,32m$ reached $70°C$ in summer and $26°C$ in winter. Since then, the idea of artificially create salinity gradient in ponds for the collection and storage of solar energy. The salinity gradient solar pond constitutes of three superposed zones.

- An upper convective zone of a few centimeters thickness UCZ (Upper Convective Zone). This zone is made up of very low salt water.
- A bottom convective zone LCZ (: Lower convective zone) of greater thickness is generally saturated with salt, and therefore the densest.
- These last two areas are separated by a third zone called a non-convective zone NCZ (for: Non Convective Zone) or salinity gradient zone. This zone is itself made up of several sublayer of different salinities, which prevents any natural convection due to increasing density with depth.

Firstly, when solar radiation reaches the bottom of the pond it heats the lower convective layer of the pond, the density of the latter must therefore decrease due to thermal expansion, on the other hand, because of its very high salinity, its density remains however large compared to higher layers, likewise, the salinity gradient which exists in the non-convective zone is favorable to avoid any convection current natural. Several works have studied the different aspects of this means of storage as well as the use of solar energy. From most interesting aspects, we can mention here the importance of the NCZ and its temperature gradient. Different salts have been used for the purpose improve the performance of the solar pond. Since, the idea to artificially create salinity gradient solar ponds has begun. The depletion of Several works have shown that it is possible to use the solar energy by transforming it into different forms: electrical, thermal, chemical, etc. .. Despite this abundance and availability, solar energy could not replace traditional energy sources due to the high cost of storage [2].

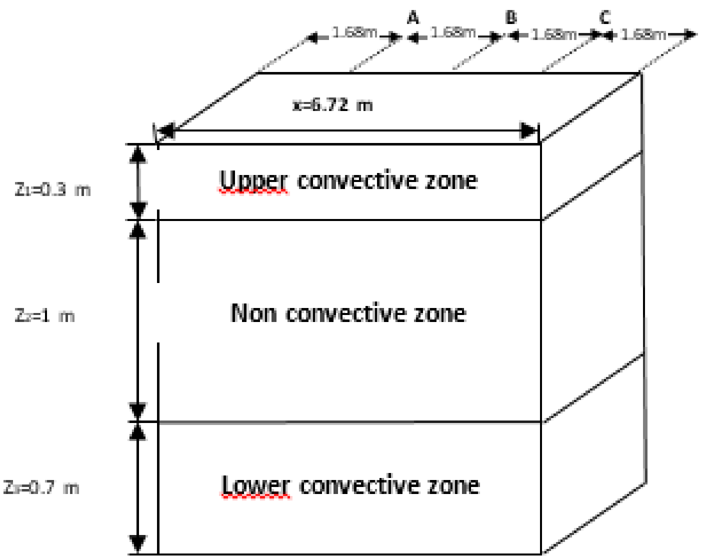

FIGURE 1. Scheme showing the three zones of a solar pond

Salinity gradient solar ponds may be the best mean to capture and store solar energy especially for a relatively long period in thermal form and at lower cost. A solar pond consists of three zones as illustrated in1. The bottom of this zone is painted black to have a maximum absorption coefficient. It is from this zone that the heat is extracted through hot water and sent towards the exchangers for various applications such as air conditioning, power generation, desalination, etc... In most studies solar ponds modeling is carried out using one-dimensional mathematical model, in other words, the heat diffusion is assumed only in the vertical direction while keeping the temperature along a layer constant. But, in our case, both the diffusion of horizontal and vertical heat was taken into account and the results of numerical simulation have shown that the difference of the temperature within the same layer of NCZ is significant and can reach $5°C$ during one season. This result shows the important role of two-dimensional modeling in solving the problem numerically. It should be noted that the experimental solar pond located at the coordinates $36°54'15''$ North and $7°45'07$" east, with a depth of $2m$, dug into the ground. The walls are covered with a PVC liner in order to minimize heat loss. Thermocouples Chrome-Alumel (K type) are designed and calibrated in the laboratory and spaced in the wall of the pond with an interval of $10cm$. To our knowledge, in previous studies, no attempts are made to solve numerically the thermal performance of salt-gradient solar ponds by using the ADI (Alternating Directions Implicit) method. SuraTundee et al. [1], Murthy et al. [3], Saxena et al. [4], and Jaeferzadeh et al. [5] studied the one-dimensional governing equation of heat conduction with solar absorption inside the solar pond. The prediction of the evolution of the temperature and salinity profiles was carried out in transient behavior. Few works, Ben Mansour et al. [6], Mazidi et al. [7], Boudiaf et al. [8] and Refaee et al. [9], have studied numerically the thermal performance, i.e, the distribution of temperature and salinity using two-dimensional transient model taking into account the influence of external factors. A Finite-Volume method has been used therein to solve a two-dimensional heat and mass transfer model. They used computer software to compute the temperature profiles. We also quote the recent work of Berkani et al. using the Crank Nicholson scheme [10]. The essential objective of this study is the numerical simulation of two solar ponds of the same dimensions and exposed to the same meteorological and weather conditions. In this direction, the comparison between these two ponds must concern the temperature profile in order to ultimately show the role that the nanoparticles of the conductive metal such as copper can play in the rise of temperature at the level of the storage zone. For this purpose, two solar ponds were studied numerically the first one is ordinary solar pond without the the presence of Cu (copper) nanoparticles, however the second one contains $28.5kg$ (concetration of $0,09\%$) is used to study the inflence of the great thermal conductivity (and therefore the fluid thermal conductivity) of nanoparticles on the energy performance of this latter pond. The essential contribution of this work includes the following points:

- The use for the first time of meteorological data from the city of Annaba (Algeria).
- Demonstration of the influencing role that copper nanoparticles can play on the temperature profile.
- The ADI method used in the numerical resolution of the mathematical problem finds its first application in a real solar pond.

It is important to mention that the statistical data used concerning the ambient temperatures and the intensity of the local solar radiation were provided by the meteorological station of the city of Annaba for the last 10 years. And finally the convergence, the consistency, and the stability were taken into account to validate the method of numerical resolution.

2. DESCRIPTION AND MATHEMATICAL FORMULATION OF THE PROBLEM

In this study, we use a two-dimensional mathematical model with an initial condition and four boundary conditions. In addition, the discrete model uses an implicit scheme similar to the prediction-correction type called ADI (Alternating Direction Implicit) that falls into the category of fractional step methods or splitting methods which have important qualitative properties such as stability, accuracy and convergence. The time and spatial discretization steps are taken successively as the $\frac{1}{4}$, $\frac{1}{8}$ and $\frac{1}{16}$ of the total duration 28 days, the horizontal length (6.72 meters along OX of the basin) and the thickness (vertical) of the NCZ (1 meter along the depth OZ) respectively. Thus:

$$\Delta x = \Delta z = \Delta t = \frac{1}{4}, \Delta x = \Delta z = \Delta t = \frac{1}{8}, \Delta x = \Delta z = \Delta t = \frac{1}{16}.$$

We consider the following in salinities mass percentages:

$$S = 5.5\%; S = 11\%; S = 16.5\%; S = 22\%.$$

An increasingly fine mesh is considered taking into account the change in physical properties and thermo-physics. To our knowledge, it is for the first time that the convergence, stability and consistency properties have been used in the study of two-dimensional mathematical modeling of heat transfer phenomena in the salt gradient solar pond using climate data for Annaba city (Algeria). The assumptions of this model are:

- The heat loss through the vertical walls along the OY axis are neglected.
- The thermo-physical properties vary from one layer to another.
- The total attenuation of solar radiation in the area is described by Giestas et al. model [11].

By applying the energy balance to a control volume $\Delta x \Delta y \Delta z$ from the non convective zone fig 2 we get Accumulated energy= output thermal flux- input thermal flux + generated energy

$$
\begin{aligned}
& (q_{t+\Delta t} - q_t) \times x.\Delta y.\Delta z = (Q_x - Q_(x + \Delta x)).\Delta y.\Delta z.\Delta t \\
(2.1) \qquad + \quad & (Q_z - Q_(z + \Delta z)).\Delta x.\Delta y.\Delta t + (E_z - E_(z + \Delta z)).\Delta x.\Delta y.\Delta t
\end{aligned}
$$

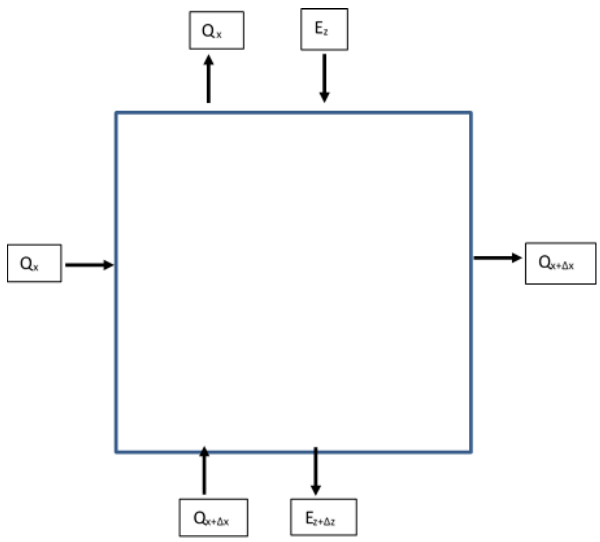

FIGURE 2. heat balance over square control volume

Dividing equation 2.5 by $\Delta t.\Delta x.\Delta y.\Delta z \neq 0$ we get:

$$\frac{(q_{t+\Delta t} - q_t)}{\Delta t} = \frac{(Q_x - Q_{x+\Delta x})}{\Delta x} + \frac{(Q_z - Q_(z + \Delta z))}{\Delta z} + \frac{E_z - E_{z+\Delta z)}}{\Delta z}. \tag{2.2}$$

By application of 1st order Taylor series the equation 2.2 becomes:

$$\begin{aligned} \left[\frac{\left(q_t + \frac{\partial q_t}{\partial t} - q_t\right)}{\Delta t}\right] &= \left[\frac{\left(Q_x - \left(Q_x + \frac{\partial Q_x}{\partial x}\right)\Delta x\right)}{\Delta x}\right] \\ &+ \left[\frac{\left(Q_z - \left(Q_z + \frac{\partial Q_z}{\partial z}\right)\Delta z\right)}{\Delta z}\right] \\ &+ \left[\frac{\left(E_z - \left(E_z + \frac{\partial E_z}{\partial z}\right)\Delta z\right)}{\Delta z}\right]. \end{aligned} \tag{2.3}$$

Taking the limits of each terms when $\Delta x, \Delta y, \Delta z, \Delta t$ tends toward 0 equation 2.3 become:

$$\frac{\partial q_t}{\partial t} = -\frac{\partial Q_x}{\partial x} - \frac{\partial Q_z}{\partial z} - \frac{dE_z}{dz}, \tag{2.4}$$

where:

$$\frac{\partial q_t}{\partial t} = \rho C_p \frac{\partial T}{\partial t}; \quad Q_x = -k_x \frac{\partial T}{\partial x}; \quad Q_z = -k_z \frac{\partial T}{\partial z}.$$

By replacing q, Q_x, Q_y, Q_z by their expression 2.4 in equation we get:

$$\rho C_p \frac{\partial T}{\partial t} = \frac{\partial}{\partial x}\left(k_x \frac{\partial T}{\partial x}\right) + \frac{\partial}{\partial z}\left(k_z \frac{\partial T}{\partial z}\right) - \frac{dE}{dz}.$$

As thermal conductivity k is the same in all direction $k_x = k_z = k$, the last equation becomes:

$$\frac{\partial T}{\partial t} = \frac{k}{\rho C_p}\left(\frac{\partial^2 T}{\partial X^2} + \frac{\partial^2 T}{\partial Z^2}\right) - \frac{1}{\rho C_p}\frac{dE}{dZ}. \tag{2.5}$$

The thermo-physical properties such as thermal conductivity k, the density ρ, specific heat C_P and solar radiation E change from one layer to another according to the following formulae:

- The thermal conductivity k is given by the following formula [5]

$$k = 0,553 - 0,0000813S + 0,0008(T - 20). \tag{2.6}$$

- The density ρ is given by Perry [12]

$$\rho = 998 - 0.4(T - 293.15) + 650.s. \tag{2.7}$$

- The absorption of solar radiation by the pond E is given by [11]

$$E = E_s e^{-\mu z}. \tag{2.8}$$

Here, it is assumed that the water is slightly turbid corresponding to an extinction coefficient $\mu = 0.5m-1$ for a depth Z. The specific heat $_CP$ expressed as a function of temperature is given by the following correlation [12]

$$C_p = 0.0048s^2 + 4.396s + 4180. \tag{2.9}$$

2.1. **Initial and boundary conditions.** The resolution of this equation requires the determination of initial and boundary conditions. In our case we have a single initial condition and four boundary conditions. Initial condition:

$$\text{At } t = 0, T(x, z, 0) = T_a, \tag{2.10}$$

where T_a is the constant ambient temperature.

Boundary conditions:

(1)

$$\text{At } z = z_1, T(x, z_1, t) = T_a. \tag{2.11}$$

(2) At the interface $z = z_1 + z_2$, the temperature is calculated on the basis of energy balance applied to the LCZ:

$$z_3 \rho C_p \frac{\partial T}{\partial t} = -k \frac{\partial T}{\partial z} + E_{LCZ} - Q_{out}, \tag{2.12}$$

where E_{LCZ} represents the insolation entering the storage zone LCZ and Q_out represents the heat loss from the storage zone LCZ.

(3) At $x = 0$, the temperature is calculated from the following equation:

$$-k \frac{\partial T}{\partial x}|_{x=0} = h(T - T_a). \tag{2.13}$$

(4) At $x = L$, the temperature is calculated from the following equation:

$$-k \frac{\partial T}{\partial x}|_{x=L} = h(T - T_a), \tag{2.14}$$

where h is the convection heat transfer coefficient between the wall of the pond and the air. This is assessed to be approximately $20W/m2 \cdot {}^\circ C$ [11]. k represents the thermal conductivity of water.

3. DISCRETISATION OF THE PROBLEM

The ADI method is a 2 steps implicit scheme of prediction-correction type where, on one hand, the backward implicit Euler scheme is used for prediction on a discretization temporal step of $\frac{\Delta t}{2}$ in the horizontal direction Ox, and, on the other hand, the forward Euler implicit scheme is used for correction along the depth Z.

Dividing the horizontal spatial domain $[0, L] = [0, 6.72m]$ into M sections, having each a length of $\Delta x = \frac{L}{M} = \frac{6.72}{M}$ and the vertical spatial domain $[0, Z2] = [0, 1]$ into N sections, having each a length of $\Delta z = \frac{Z_2}{N} = \frac{1m}{N}$.

The time domain $[0, T] = [0, 28\text{days}]$ is divided into P segments, each of duration $\Delta t = \frac{T}{p} = \frac{28\text{days}}{p}$.

Letting $x = i\Delta x$ for $i = 1, 2, \ldots, M$, $Z = j\Delta Z$ for $j = 1, 2, \ldots, N$ and $t = n\Delta t$ for $n = 1, 2, \ldots, P$ Equation (1) can be rewritten as follows:

step 1:

$$\frac{T_{i,j}^{n+\frac{1}{2}} - T_{i,j}^{n}}{\frac{\Delta t}{2}} = \frac{k}{\rho C_p}\left[\frac{\delta_x^2}{\Delta x^2}T_{i,j}^{n+\frac{1}{2}} + \frac{\delta_{z^2}}{\Delta Z^2}T_{i,j}^{n}\right] - \frac{1}{\rho C_p}\left[\frac{E_{i,j+1}^{n} - E_{i,j-1}^{n}}{2\Delta Z}\right]. \tag{3.1}$$

step2:

$$\frac{T_{i,j}^{n+1} - T_{i,j}^{n+\frac{1}{2}}}{\frac{\Delta t}{2}} = \frac{k}{\rho C_p}\left[\frac{\delta_x^2}{\Delta x^2}T_{i,j}^{n+\frac{1}{2}} + \frac{\delta_{z^2}}{\Delta Z^2})T_{i,j}^{n+1}\right] - \frac{1}{\rho C_p}\left[\frac{E_{i,j+1}^{n+\frac{1}{2}}}{-}E_{i,j-1}^{n+\frac{1}{2}}2\Delta Z/\right] \tag{3.2}$$

with the notation:

$$\delta_x^2 T_{i,j}^{n} = T_{i-1,j}^{n} - 2T_{i,j}^{n} + T_{i+1,j}^{n} \tag{3.3}$$

$$\delta_z^2 T_{i,j}^{n} = T_{i,j-1}^{n} - 2T_{i,j}^{n} + T_{i,j+1}^{n} \tag{3.4}$$

δ_x^2andδ_z^2 are the central difference operators in x and z direction respectively Putting $r_x = \frac{k\Delta t}{(\rho C_p \Delta x^2)}$ and $r_z = \frac{k\Delta t}{(\rho C_p \Delta z^2)}$, we get:

$$T_{i,j}^{n+\frac{1}{2}} = T_{i,j}^{n} + \frac{r_z}{2}\delta_z^2 T_{i,j}^{n} + \frac{r_x}{2}\delta_x^2 T_{i,j}^{n+\frac{1}{2}} - r_z\frac{\Delta Z}{4K}\left[E_{i,j+1}^{n} - E_{i,j-1}^{n}\right] \tag{3.5}$$

$$T_{i,j}^{n+1} = T_{i,j}^{n+\frac{1}{2}} + \frac{r_x}{2}\delta_x^2 T_{i,j}^{n+\frac{1}{2}} + \frac{r_z}{2}\delta_z^2 T_{i,j}^{n+1} - r_z\frac{\Delta Z}{4k}\left[E_{i,j+1}^{n+\frac{1}{2}} - E_{i,j-1}^{n+\frac{1}{2}}\right] \tag{3.6}$$

After discretization, equations (3.5) and (3.6) can be rewritten as below:

$$
\begin{aligned}
&-\frac{r_x}{2}T_{i-1,j}^{n+\frac{1}{2}}+(1+r_x)T_{i,j}^{n+\frac{1}{2}}-\frac{r_x}{2}T_{i+1,j}^{n+\frac{1}{2}}\\
&=\frac{r_z}{2}T_{i,j-1}^{n}+(1-r_z)T_{i,j}^{n}+\frac{r_z}{2}T_{i,j+1}^{n}-r_Z\frac{\Delta Z}{4k}\left[E_{i,j+1}^{n}-E_{i,j-1}^{n}\right]
\end{aligned}
\tag{3.7}
$$

$$
\begin{aligned}
&-\frac{r_z}{2}T_{i,j-1}^{n+1}+1+r_zT_{i,j}^{n+1}-\frac{r_z}{2}T_{i,j+1}^{n+1}\\
&=\frac{r_x}{2}T_{i-1,j}^{(}n+1/2)+1-r_xT_{i,j}^{n+\frac{1}{2}}+\frac{r_x}{2}T_{i+1,j}^{n+\frac{1}{2}}-\frac{r_Z\Delta Z}{4k}\left[E_{i,j+1}^{n+\frac{1}{2}}-E_{i,j-1}^{n+\frac{1}{2}}\right].
\end{aligned}
\tag{3.8}
$$

Thus, with the initial condition at $(n=0)$, $T_{i,j}^{0}=T_a$ for $i=0,1,2\ldots,M$,$j=0,1,2,\ldots,N$, and assuming that the solution $T_{i,j}^{n}$, for $i=0,1,2,\ldots,M$ and $j=0,1,2,\ldots,N$, has been computed, equation (3.4) is being used to compute $T_{i,j}^{n+\frac{1}{2}}$ at all interior points, for $i=0,1,2,\ldots,M-1$ and $j=0,1,2,\ldots,N-1$. The matrix form of the general equation (3.4) is rewritten as:

$$
[I+A_x]T_j^{n+\frac{1}{2}}=f_{z,j}^{n}+S_j^{n},
\tag{3.9}
$$

where I is the identity matrix and $T_j^{n+\frac{1}{2}}$ is the temperature vector at time $(n+\frac{1}{2})$ and is given by:

$$
T_j^{n+\frac{1}{2}}=\begin{bmatrix} T_{1,j}^{n+\frac{1}{2}}\\ T_{2,j}^{n+\frac{1}{2}}\\ \vdots\\ T_{M-1,j}^{n+\frac{1}{2}}\end{bmatrix},
$$

A_x is an $(M-1)(N-1)\times(M-1)(N-1)$ block tri-diagonal matrix and is given by:

$$
A_x=\begin{bmatrix}
2D_x & -D_x & 0 & \ldots & \ldots & 0\\
-D_x & 2D_x & -D_x & \ldots & \ldots & \ldots\\
0 & -D_x & 2D_x & -D_x & \ldots & \ldots\\
\ldots & \ldots & \ddots & \ddots & \ldots & \ldots\\
\ldots & \ldots & \ddots & \ddots & \ddots & \ldots\\
0\ldots & \ldots & \ldots & -D_x & 2D_x &
\end{bmatrix},
$$

where

$$D_x = \begin{bmatrix} \frac{r_x}{2} & 0 & \dots & \dots & 0 \\ 0 & \dots & \dots & \dots & \dots \\ \vdots & \dots & \dots & \dots & \dots \\ \vdots & \dots & \dots & \dots & \dots \\ 0 & \dots & \dots & \dots & \dots \end{bmatrix},$$

D_x are $(M-1) \times (M-1)$ diagonal matrices.

$$f_{z,j}^n = \begin{bmatrix} T_{1,j}^n + \frac{r_z}{2}(T_{1,j-1}^n - 2T_{1,j}^n + T_{1,j+1}^n) \\ T_{2,j}^n + \frac{r_z}{2}(T_{2,j-1}^n - 2T_{2,j}^n + T_{2,j+1}^n) \\ \vdots \\ \vdots \\ T_{M-1,j}^n + \frac{r_z}{2}(T_{M-1,j-1}^n - 2T_{M-1,j}^n + T_{M-1,j+1}^n) \end{bmatrix},$$

Further, S_j^n is the source term at time n depending only on the layer position in the pond and is given by:

$$S_j^n = -r_z \frac{\Delta Z}{4k} = \begin{bmatrix} C_z & 0 & \dots & \dots & 0 \\ 0 & \dots & \dots & \dots & \\ \vdots & \vdots & \vdots & \vdots & \vdots \\ 0 & \dots & \dots & \dots & C_z \end{bmatrix},$$

where

$$C_z = \begin{bmatrix} -1 & 0 & 1 & 0 & \dots & 0 \\ 0 & \dots & \dots & \dots & \dots & \vdots \\ \vdots & \vdots & \vdots & \vdots & \vdots & \vdots \\ 0 & \dots & \dots & -1 & 0 & -1 \end{bmatrix}.$$

Equation (3.8) is used to compute $T_{i,j}^{n+1}$ at all interior points for $i = 0, 1, 2, \dots, M-1$ and $j = 0, 1, 2, \dots, N-1$. The matrix form of the general equation (3.8) can be written as follows:

$$[I + A_z]T_i^{n+1} = f_{x,i}^{n+\frac{1}{2}} + S_j^{n+\frac{1}{2}}, \tag{3.10}$$

T_i^{n+1} is the temperature vector at time $(n+1)$ and is given by:

$$T_i^{n+1} = \begin{bmatrix} T_{i,1}^{n+1} \\ T_{i,2}^{n+1} \\ \vdots \\ T_{i,N-1}^{n+1} \end{bmatrix},$$

$S_j^{n+\frac{1}{2}}$ is the source term at time $n+\frac{1}{2}$ and $f_{x,i}^{n+\frac{1}{2}}$ is an $(M-1)(N) \times (M-1)(N)$ block tridiagonal matrix.

4. NUMERICAL RESOLUTION

To solve numerically the model, by fixing j and varying i from 1 to 4, we get two systems of equations where each includes 16 equations with 24 unknowns. The first system has as unknowns the temperature at time $n+\frac{1}{2}$ that will be solved as a function of temperature at time n and the second system includes as unknowns the temperature at time $n+1$ which will be solved as a function of the temperature at time $n+\frac{1}{2}$. So equation (3.7) gives the following expression:

$$[P]\begin{bmatrix} T_{0,j}^{n+\frac{1}{2}} \\ T_{1,j}^{n+\frac{1}{2}} \\ T_{2,j}^{n+\frac{1}{2}} \\ T_{3,j}^{n+\frac{1}{2}} \\ T_{4,j}^{n+\frac{1}{2}} \\ T_{5,j}^{n+\frac{1}{2}} \end{bmatrix} = \frac{r_z}{2}[I]\begin{bmatrix} T_{1,j-1}^{n} \\ T_{2,j-1}^{n} \\ T_{3,j-1}^{n} \\ T_{4,j-1}^{n} \end{bmatrix} + (1-r_z)[I]\begin{bmatrix} T_{1,j}^{n} \\ T_{2,j}^{n} \\ T_{3,j}^{n} \\ T_{4,j}^{n} \end{bmatrix} + \frac{r_z}{2}[I]\begin{bmatrix} T_{1,j+1}^{n} \\ T_{2,j+1}^{n} \\ T_{3,j+1}^{n} \\ T_{4,j+1}^{n} \end{bmatrix}$$

$$+ \quad r_z\frac{\Delta Z}{4k}[I]\begin{bmatrix} E_{1,j-1}^{n} \\ E_{2,j-1}^{n} \\ E_{3,j-1}^{n} \\ E_{4,j-1}^{n} \end{bmatrix} - r_z\frac{\Delta Z}{4k}[I]\begin{bmatrix} E_{1,j+1}^{n} \\ E_{2,j+1}^{n} \\ E_{3,j+1}^{n} \\ E_{4,j+1}^{n} \end{bmatrix}$$

with

$$[P_x] = \begin{bmatrix} -\frac{r_x}{2} & (1+r_x) & \frac{r_x}{2} & 0 & 0 & 0 \\ 0 & -\frac{r_x}{2} & (1+r_x) & -\frac{r_x}{2} & 0 & 0 \\ 0 & 0 & -\frac{r_x}{2} & (1+r_x) & -\frac{r_x}{2} & 0 \\ 0 & 0 & 0 & -\frac{r_x}{2} & (1+r_x) & -\frac{r_x}{2} \end{bmatrix}; \ [I]\begin{bmatrix} 1 & 0 & 0 & 0 \\ 0 & 1 & 0 & 0 \\ 0 & 0 & 1 & 0 \\ 0 & 0 & 0 & 1 \end{bmatrix}.$$

Equation (3.8) gives:

$$
[Q_x]\begin{bmatrix} T_{0,j}^{n+\frac{1}{2}} \\ T_{1,j}^{n+\frac{1}{2}} \\ T_{2,j}^{n+\frac{1}{2}} \\ T_{3,j}^{n+\frac{1}{2}} \\ T_{4,j}^{n+\frac{1}{2}} \\ T_{5,j}^{n+\frac{1}{2}} \end{bmatrix} = -\frac{r_z}{2}[I]\begin{bmatrix} T_{1,j-1}^{n} \\ T_{2,j-1}^{n} \\ T_{3,j-1}^{n} \\ T_{4,j-1}^{n} \end{bmatrix} + (1+r_z)[I]\begin{bmatrix} T_{1,j}^{n} \\ T_{2,j}^{n} \\ T_{3,j}^{n} \\ T_{4,j}^{n} \end{bmatrix} - \frac{r_z}{2}[I]\begin{bmatrix} T_{1,j+1}^{n} \\ T_{2,j+1}^{n} \\ T_{3,j+1}^{n} \\ T_{4,j+1}^{n} \end{bmatrix}
$$

$$
+ \; r_z\frac{\Delta Z}{4k}[I]\begin{bmatrix} E_{1,j-1}^{n+\frac{1}{2}} \\ E_{2,j-1}^{n+\frac{1}{2}} \\ E_{3,j-1}^{n+\frac{1}{2}} \\ E_{4,j-1}^{n+\frac{1}{2}} \end{bmatrix} - r_z\frac{\Delta Z}{4k}[I]\begin{bmatrix} E_{1,j+1}^{n} \\ E_{2,j+1}^{n} \\ E_{3,j+1}^{n} \\ E_{4,j+1}^{n} \end{bmatrix},
$$

with

$$
Q_x = \begin{bmatrix} \frac{r_x}{2} & (1-r_x) & \frac{r_x}{2} & 0 & 0 & 0 \\ 0 & \frac{r_x}{2} & (1-r_x) & \frac{r_x}{2} & 0 & 0 \\ 0 & 0 & \frac{r_x}{2} & (1-r_x) & \frac{r_x}{2} & 0 \\ 0 & 0 & 0 & \frac{r_x}{2} & (1-r_x) & \frac{r_x}{2} \end{bmatrix}.
$$

Equation (3.5) gives a system of 16 equations with 24 unknowns (Fig. 3) by varying i from 1 to 4 for each value of j which is varied in its turn from 1 to 4.

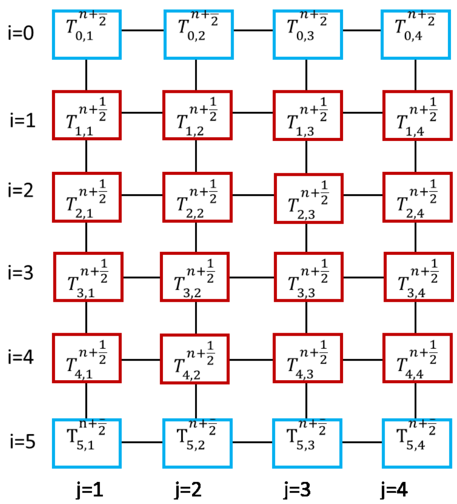

FIGURE 3. Temperature distribution for a given calculation at the first step

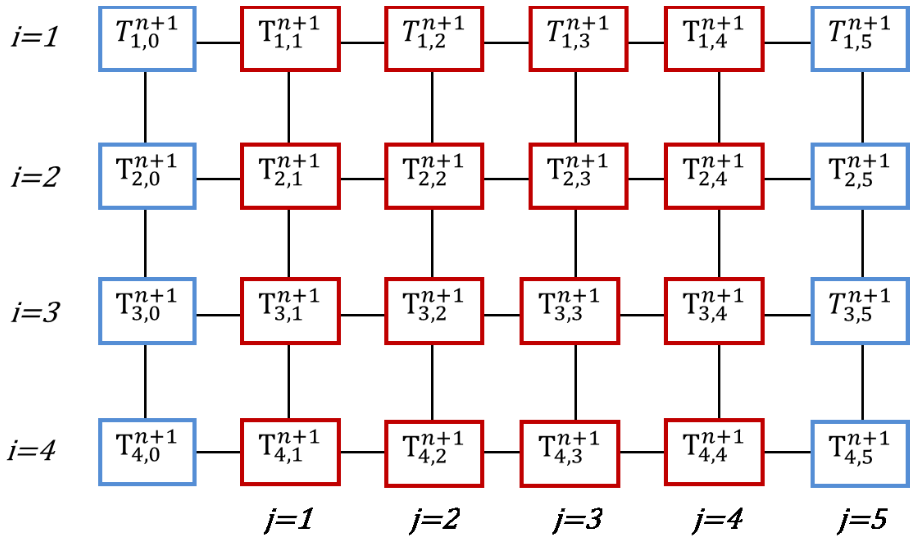

FIGURE 4. Temperature distribution for a given calculation at the second step

Equation (3.8) gives a system of 16 equations with 24 unknowns (Fig. 4) by varying i from 1 to 4 for each value of j which is varied in its turn from 1 to 4.

4.1. **Incorporation of the initial and boundary conditions.** The use of initial and boundary condition equations reduces the number of unknowns to 16 in equations (3.7) and (3.8):

- At the pond water surface, the temperatures

$$T_{0,1}^{n+\frac{1}{2}}, \quad T_{0,2}^{n+\frac{1}{2}}, \quad T_{0,3}^{n+\frac{1}{2}}, \quad T_{0,4}^{n+\frac{1}{2}}$$

  are equal to the ambient temperature by the application of the first boundary condition.
- At the interface $z = z_1 + z_2$, the temperatures

$$T_{51}^{n+\frac{1}{2}}, \quad T_{52}^{n+\frac{1}{2}}, \quad T_5 3^(n + 1/2), \quad T_{54}^{n+\frac{1}{2}}$$

  are calculated by the 2nd boundary condition and from the discretization of equation (2.12):

$$\frac{T_{i,j}^(n+\frac{1}{2}) - T_{i,j}^n}{\frac{\Delta t}{2}} = \frac{-k}{\rho Z_3 C_p}\left[\frac{T_{i,j}^n - T_{i,j-1}^n}{\Delta Z}\right] + \frac{E_{LCZ} - Q_{out}}{\rho Z_3 C_p}. \tag{4.1}$$

- At the bottom of the basin i.e. $i = 5$, we obtain

$$T_{5,j}^{n+\frac{1}{2}} = T_{5,j}^{n}\left[1 + \frac{-k\Delta t}{2\rho C_p \Delta z Z_3}\right] - \frac{k\Delta t T_{5,j-1}^{n}}{2\rho C_p \Delta z Z_3} + \frac{((E_{LCZ} - Q_{OUT})\Delta t)}{2\rho C_p Z_3}. \tag{4.2}$$

In our case $T_{5,j}^n = T_{4,j}^n$ since the temperature of the LCZ is equal to the temperature of the last layer NCZ. Q_{out} represents about 14% of the incident energy [12].

- At $x = 0$, i.e. i varying from 1 to 4, the temperatures

$$T_{1,0}^{n+1},\quad T_{2,0}^{n+1},\quad T_{3,0}^{n+1},\quad T_{4,0}^{n+1},$$

are determined by the 3rd boundary condition and from the discretization of equation (2.13):

$$T_(i,0)^(n+1) = T_(i-1,0)^(n+1)[(k-h\Delta x)/k] + h\Delta x/kT_a withT_0, 0 = T_a. \tag{4.3}$$

- At $x = L$, which corresponds to $j = 5$, the temperatures

$$T_{1,5}^{n+1},\quad T_{2,5}^{n+1},\quad T_{3,5}^{n+1},\quad T_{4,5}^{n+1},$$

are determined by applying the 4th boundary condition and from the discretization of the equation (2.14) we get:

$$T_{i,5}^{n+1} = T_{i-1,5}^{n+1}\left[\frac{k - h\Delta x}{k}\right] + \frac{h\Delta x}{kT_a}. \tag{4.4}$$

Finally, by adopting the same reasoning for the second and third grids, we obtain a linear system of the form $AT = B$ where A is a sparse matrix, T is the temperature field to be determined and B is the RHS vector of the discretized equation. Equation (3.7) gives a system of equations having as unknowns the temperature at time $(n+\frac{1}{2})$ in function of temperature at time n. Equation (3.8) gives a system of equations having as unknowns the temperature at time $(n+1)$ as function of temperature at time $(n+\frac{1}{2})$. For the step $\Delta x = \Delta z = \Delta t = \frac{1}{4}$, we obtain 4×4 unknowns at time $(n+\frac{1}{2})$ and 4×4 unknowns at time $(n+1)$; for $\Delta x = \Delta z = \Delta t = \frac{1}{8}$, 8×8 unknowns at time $(n+\frac{1}{2})$ and 8×8 unknowns at time $(n+1)$, whereas, for $\Delta x = \Delta z = \Delta t = \frac{1}{16}$, this number reaches 16×16 unknowns at the time $(n+\frac{1}{2})$ and 16×16 unknowns at the time $(n+1)$. The Gauss-Seidel iterative method is used because of its high stability w.r.t rounding errors.

5. RESULTS AND DISCUSSION

5.1. Different Meshes and temperature profile.

First mesh:

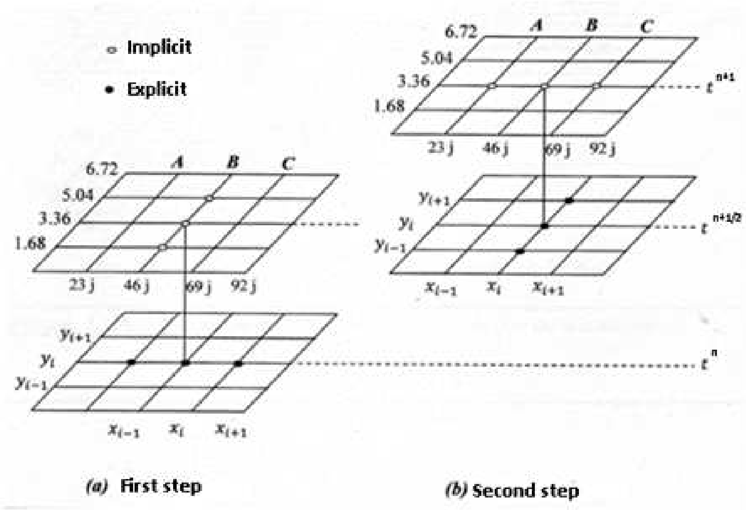

FIGURE 5. 1st mesh representation for discretization step $Deltax = \Delta y = \Delta t = \frac{1}{4}$

Second mesh:

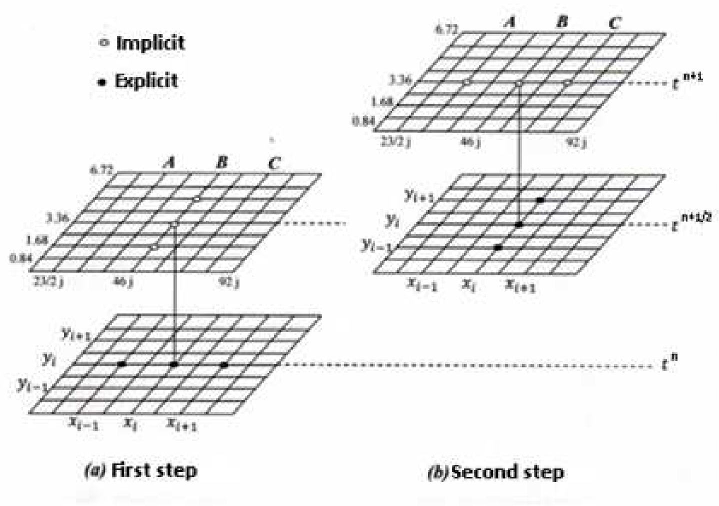

FIGURE 6. 2nd mesh representation for discretization step $\Delta x = \Delta y = \Delta t = \frac{1}{8}$

Third mesh:

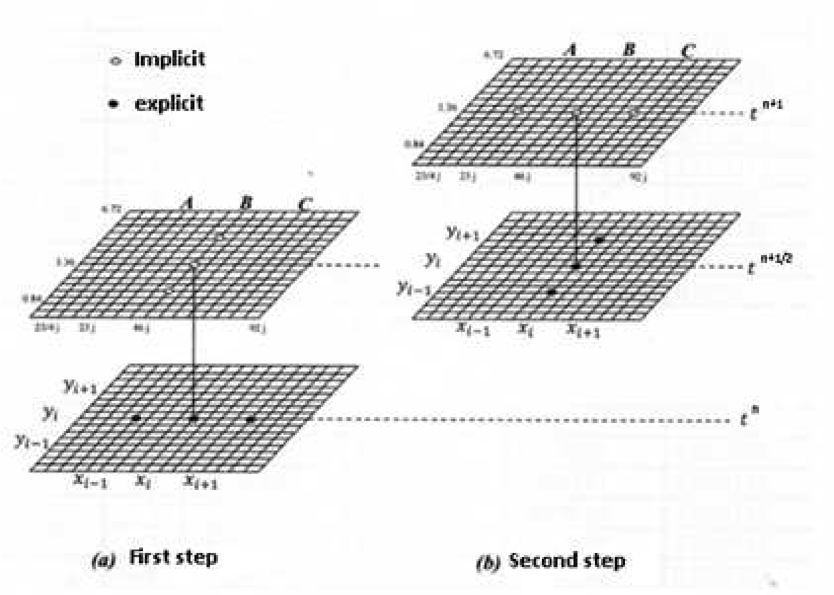

FIGURE 7. 3rd mesh representation for discretization step $\Delta x = \Delta y = \Delta t = \frac{1}{16}$

The temperature profile according to the horizontal direction ox and along the depth oz is given at the points A, B, C (Tables 1 and 2; Figures 5,6 and 7) which are located respectively at the left, middle and right of the NCZ zone.

5.2. **Discussion.** The simulation results obtained are displayed in the tables below and indicate a temperature variation along a layer. Moreover, we also observe a high and rapid heating in the central part of the pond than at its periphery this can be explained by heat loss at the walls and, according to the calculations, the upper part of the NCZ heats up less than its lower part. For a given layer the horizontal temperature range can reach $5°C$, confirming the importance of the two-dimensional treatment compared to the one-dimensional which considers the temperature as being constant in a given layer. To calculate the error, a reference solution T_{ref} has been taken as the finest mesh solution corresponding to a mesh size of $h = \frac{1}{16}$. The percentage relative error is defined by $\left|\frac{T_{ref}-T_h}{T_{ref}}\right| \times 100$. T_h is the numerical solution for a given step h. Tables 1 and 2 show that this error decreases gradually as h tends toward zero.

Table 1: Temperature evolution in the NCZ without nanoparticles

Discretisation step \ Horizontal Direction	A	B	C
After 7 days			
$\Delta x = \Delta z =$ ¼	36.232	37.696	36.413
$\Delta x = \Delta z = 1/8$	36.358	37.746	36.488
Er.rel %	0.192	0.139	0.217
$\Delta x = \Delta z = 1/16$	36.342	37.758	36.492
Relative error (%)	0.046	0.033	0.011
After 14 days			
$\Delta x = \Delta z =$ ¼	47.713	50.102	47.698
$\Delta x = \Delta z = 1/8$	47.776	50.154	47.738
Er.rel %	0.147	0.115	0.0932
$\Delta x = \Delta z = 1/16$	47.801	50.172	47.731
Relative error (%)	0.058	0.039	0.016
After 21 days			
$\Delta x = \Delta z =$ ¼	57.399	61.003	57.314
$\Delta x = \Delta z = 1/8$	57.326	61.941	57.292
Er.rel %	0.142	0.112	0.042
$\Delta x = \Delta z = 1/16$	57.338	61.924	57.281
Relative error (%)	0.023	0.030	0.021
After 28 days			
$\Delta x = \Delta z =$ ¼	68.311	73.286	68.220
$\Delta x = \Delta z = 1/8$	68.426	73.364	68.308
Er.rel %	0.187	0.117	0.143
$\Delta x = \Delta z = 1/16$	68.444	73.351	68.314
Relative error (%)	0.029	0.019	0.009

Table 2: Temperature evolution in the NCZ with nanoparticles

Discretisation step \ Horizontal Direction	A	B	C
After 7 days			
$\Delta x = \Delta z = 1/4$	41.124	42.183	41.140
$\Delta x = \Delta z = 1/8$	41.098	42.126	41.104
Er.rel %	0.161	0.331	0.223
$\Delta x = \Delta z = 1/16$	41.084	42.114	41.082
Relative error (%)	0.087	0.070	0.136
After 14 days			
$\Delta x = \Delta z = 1/4$	52.154	55.688	52.192
$\Delta x = \Delta z = 1/8$	52.111	55.620	52.134
Er.rel %	0.203	0.299	0.273
$\Delta x = \Delta z = 1/16$	52.092	55.609	52.146
Relative error (%)	0.090	0.048	0.056
After 21 days			
$\Delta x = \Delta z = 1/4$	63.001	67.143	63.128
$\Delta x = \Delta z = 1/8$	63.082	67.183	63.175
Er.rel %	0.311	0.141	0.179
$\Delta x = \Delta z = 1/16$	63.071	67.154	63.155
Relative error (%)	0.042	0.102	0.075
After 28 days			
$\Delta x = \Delta z = 1/4$	77.184	83.522	77.283
$\Delta x = \Delta z = 1/8$	77.226	83.607	77.324
Er.rel %	0.134	0.253	0.131
$\Delta x = \Delta z = 1/16$	77.238	83.626	77.348
Relative error (%)	0.038	0.056	0.076

This shows a convergence trend of the approximate solution toward the exact solution and thus corroborating the theoretical convergence result given by proposition 11.6 of the reference [13]. In the solar pond, there is a vertical and horizontal migration within the same layer under the Soret effect [14]. Vertical migration of salt is less important at the center of the basin than at the periphery. Therefore, LCZ is poorer in salt at the periphery than at the center and this helps locating the optimal point of salt injection for maintenance of the pond. This Soret effect causes non-uniform vertical salt migration. This would be a factor causing non-uniformity of natural convection flows within LCZ and can also adversely affect the physical stability of the solar pond. The temperature reaches a maximum of $80^{circ}C$ in the presence of nanoparticles and $73°C$ without their presence in the storage zone LCZ according to the conditions of the considered pond. This indicates the appropriate time to fill the pond. It should be noted that the pond containing the copper nanoparticles records a temperature of around $80°C$ compared to the pond without metal nanoparticles. We estimate that this temperature far exceeds the functional temperature, which is around $63°C$. In this work, it appears that the temperature of LCZ in locations near the NCZ-LCZ interface is not the same. This confirms that the natural convection has not the same intensity in the storage layer. The heat extraction point should be carefully chosen because the temperature is maximum at the center of the pond. The notion of convergence of a numerical scheme expresses the property of the numerical solution to tend toward the exact solution of the considered problem as the mesh size decreases. It is possible to show that the convergence is ensured under the conditions of the Lax-Richtmyer equivalence theorem [15]:

Proposition 5.1. *The numerical scheme given by (3.9) and (3.10) is both consistent and stable.*

Proof.
a) Consistency The idea behind the ADI method is to introduce intermediate calculations to go from T^n to T^{n+1} which requires only the resolution of one-dimensional problems. Equation (2.5) for the heat transfer is of the form: $\frac{\partial T}{\partial t} + LT = S$ where, the operator L is independent of time and splits up as follows:

$$L = L_1 + L_2,$$

with

$$L_1 = \frac{-k}{\rho C_p}\frac{\partial^2}{\partial X^2}; \quad L_2 = \frac{-k}{\rho C_p}\frac{\partial^2}{\partial Z^2}; \quad S = \frac{-1}{\rho C_p}\frac{dE}{dZ}.$$

Equations (5.2) and (3.2) can be rewritten respectively as

$$\begin{aligned} &\frac{2}{\Delta t}\left(T_{i,j}^{n+\frac{1}{2}} - T_{i,j}^{n}\right) - \frac{r_x}{\Delta t}\left[T_{i-1,j}^{n+\frac{1}{2}} - 2T_{i,j}^{n+\frac{1}{2}} + T_{i+1,j}^{n+\frac{1}{2}}\right] \\ &-\frac{r_z}{\Delta t}[T_{i,j-1}^{n} - 2T_{i,j}^{n} + T_{i,j+1}^{n}] = S_j^n \end{aligned} \tag{5.1}$$

(5.2)
$$\begin{aligned}&\frac{2}{\Delta t}(T_{i.j}^{n+1}-T_{i,j}^{n+\frac{1}{2}}-\frac{r_x}{\Delta t}\left[T_{i-1,j}^{n+\frac{1}{2}}-2T_{i,j}^{n+\frac{1}{2}}+T_{i+1,j}^{n+\frac{1}{2}}\right]\\&-\frac{r_z}{\Delta t}\left[T_{i,j-1}^{n+1}-2T_{i,j})^{n+1}+T_{i,j+1}^{n+1}\right]=S_j^{n+\frac{1}{2}}\end{aligned}$$

This system of equations takes the following matrix form:

$$\begin{aligned}\frac{2}{\Delta t}\left(T_{i.j}^{n+\frac{1}{2}}-T_{i.j}^{n}\right) \quad - \quad \frac{r_x}{\Delta t}&\begin{bmatrix}-2 & 1 & 0 & 0 & \dots & 0\\ 1 & -2 & 1 & 0 & \dots & \dots\\ 0 & 1 & -2 & 1 & \dots & \dots\\ \dots & \dots & \ddots & \ddots & \ddots & \dots\\ \dots & \dots & \ddots & \ddots & \ddots & 1\\ 0 & \dots & \dots & \dots & 1 & -2\end{bmatrix}T_i^{n+\frac{1}{2}}\\ - \quad \frac{r_z}{\Delta t}&\begin{bmatrix}-2 & 1 & 0 & 0 & \dots & 0\\ 1 & -2 & 1 & 0 & \dots & \dots\\ 0 & 1 & -2 & 1 & \dots & \dots\\ \dots & \dots & \ddots & \ddots & \ddots & \dots\\ \dots & \dots & \ddots & \ddots & \ddots & 1\\ 0 & \dots & \dots & \dots & 1 & -2\end{bmatrix}T_j^{n}=S_j^n\end{aligned}$$

$$\begin{aligned}\frac{2}{\Delta t}\left(T_{i.j}^{n+1}-T_{i.j}^{n+\frac{1}{2}}\right) \quad - \quad \frac{r_x}{\Delta t}&\begin{bmatrix}-2 & 1 & 0 & 0 & \dots & 0\\ 1 & -2 & 1 & 0 & \dots & \dots\\ 0 & 1 & -2 & 1 & \dots & \dots\\ \dots & \dots & \ddots & \ddots & \ddots & \dots\\ \dots & \dots & \ddots & \ddots & \ddots & 1\\ 0 & \dots & \dots & \dots & 1 & -2\end{bmatrix}T_i^{n+\frac{1}{2}}\\ - \quad \frac{r_z}{\Delta t}&\begin{bmatrix}-2 & 1 & 0 & 0 & \dots & 0\\ 1 & -2 & 1 & 0 & \dots & \dots\\ 0 & 1 & -2 & 1 & \dots & \dots\\ \dots & \dots & \ddots & \ddots & \ddots & \dots\\ \dots & \dots & \ddots & \ddots & \ddots & 1\\ 0 & \dots & \dots & \dots & 1 & -2\end{bmatrix}T_j^{n+1}=S_j^{n+\frac{1}{2}}\end{aligned}$$

Letting

$$V_1 = -\frac{r_x}{\Delta t}\begin{bmatrix} -2 & 1 & 0 & 0 & \dots & 0 \\ 1 & -2 & 1 & 0 & \dots & \dots \\ 0 & 1 & -2 & 1 & \dots & \dots \\ \dots & \dots & \ddots & \ddots & \ddots & \dots \\ \dots & \dots & \ddots & \ddots & \ddots & 1 \\ 0 & \dots & \dots & \dots & 1 & -2 \end{bmatrix}$$

and

$$V_2 = -\frac{r_z}{\Delta t}\begin{bmatrix} -2 & 1 & 0 & 0 & \dots & 0 \\ 1 & -2 & 1 & 0 & \dots & \dots \\ 0 & 1 & -2 & 1 & \dots & \dots \\ \dots & \dots & \ddots & \ddots & \ddots & \dots \\ \dots & \dots & \ddots & \ddots & \ddots & 1 \\ 0 & \dots & \dots & \dots & 1 & -2 \end{bmatrix}$$

$\square$

The scheme of alternating directions becomes:

$$\frac{2}{\Delta t}\left(T^{n+\frac{1}{2}} - T^n\right) + V_1 T^{n+\frac{1}{2}} + V_2 T^n - S_j^n = 0, \tag{5.3}$$

$$\frac{2}{\Delta t}\left(T^{n+1} - T^n\right) + V_1 T^{n+\frac{1}{2}} + V_2 T^{n+1} - S_j^{n+\frac{1}{2}} = 0, \tag{5.4}$$

where V_1 and V_2 are matrices associated with the approximate operators of L_1 and L_2 Determining the order of convergence with respect to the space equations (5.1) and (5.2) can be written in the following form:

$$\begin{aligned} &\frac{T_{i.j}^{n+\frac{1}{2}} - T_{i.j}^n}{\Delta t} + \frac{r_x}{2\Delta t}\left[-T_{i-1,j}^{n+\frac{1}{2}} + 2T_{i,j}^{n+\frac{1}{2}} - T_{i+1,j}^{n+\frac{1}{2}}\right] \\ &+\frac{r_z}{2\Delta t}[-T_{i,j-1}^n + 2T_{i,j}^n - T_{i,j+1}^n] - \frac{S_j^n}{2} = 0, \end{aligned} \tag{5.5}$$

$$\begin{aligned} &\frac{T_{i.j}^{n+1} - T_{i.j}^{n+\frac{1}{2}}}{\Delta t} + \frac{r_x}{2\Delta t}\left[-T_{i-1,j}^{n+\frac{1}{2}} + 2T_{i,j}^{n+\frac{1}{2}} - T_{i+1,j}^{n+\frac{1}{2}}\right] \\ &+\frac{r_z}{2\Delta t}[-T_{i,j-1}^n + 2T_{i,j}^{n+1} - T_{i,j+1}^{n+1}] - \frac{S_j^{n+\frac{1}{2}}}{2} = 0. \end{aligned} \tag{5.6}$$

Substituting r_x and r_z with their expression, we obtain:

$$\begin{aligned}\frac{T_{i,j}^{n+\frac{1}{2}} - T_{i,j}^{n}}{\Delta t} \quad &+ \quad \frac{k}{2\rho C_p(\Delta x)^2}\left[-T_{i-1,j}^{n+\frac{1}{2}} + 2T_{i,j}^{n+\frac{1}{2}} - T_{i+1,j}^{n+\frac{1}{2}}\right] \\ &+ \quad \frac{k}{2\rho C_p(\Delta z)^2}\left[-T_{i,j-1}^{n} + 2T_{i,j}^{n} - T_{i,j+1}^{n}\right] - \frac{S_j^n}{2} = 0\end{aligned} \tag{5.7}$$

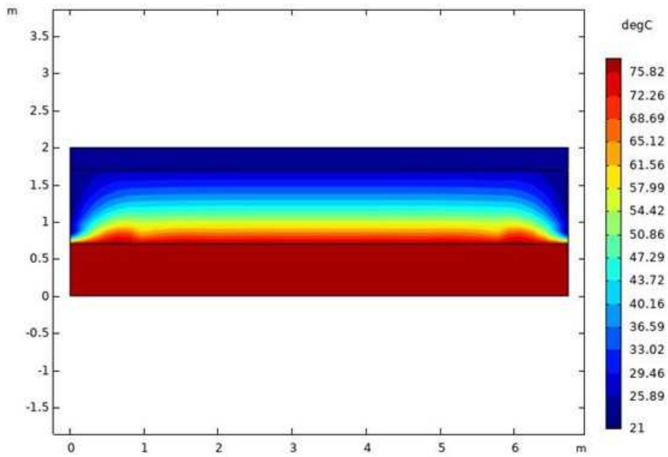

FIGURE 8. Temperature profile without the presence of metallic nanoparticles.

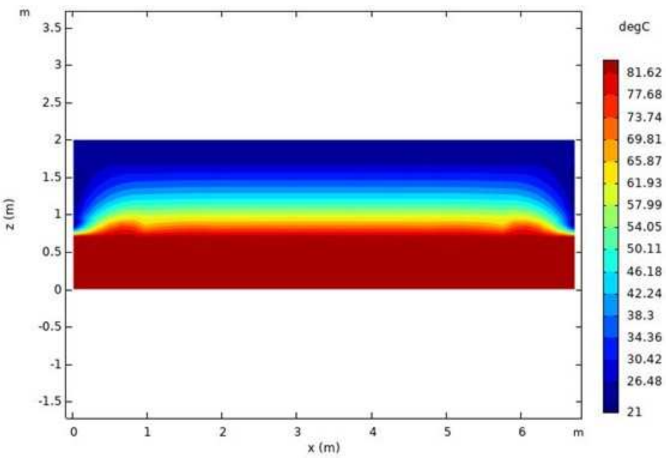

FIGURE 9. Temperature profile in the presence of metallic nanoparticles.

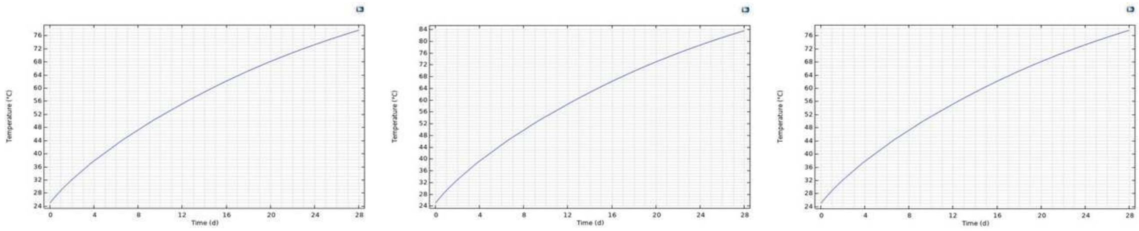

FIGURE 10. Temperature profile evolution with time during 28 days at three point A, B, C

$$\begin{aligned}(5.8)\qquad &\frac{T_{i,j}^{n+1}-T_{i,j}^{n+\frac{1}{2}}}{\Delta t}+\frac{k}{2\rho C_p(\Delta x)^2}-T_{i-1,j}^{n+\frac{1}{2}}+2T_{i,j}^{n+\frac{1}{2}}\\ &-T_{i+1,j}^{n+\frac{1}{2}}]+\frac{k}{2\rho C_p(\Delta z)^2}-T_{i,j-1}^{n+1}+2T_{i,j}^{n+1}-T_{i,j+1}^{n+1}]-\frac{S_j^{n+\frac{1}{2}}}{2}=0.\end{aligned}$$

Subtracting equation (5.8) from (5.7) gives $T_{i,j}^{n+\frac{1}{2}}$ as function of $T_{i,j}^{n}$ and $T_{i,j}^{n+1}$:

$$\begin{aligned}(5.9)\qquad T_{i,j}^{n+\frac{1}{2}}=&\frac{T_{i,j}^{n+1}+T_{i,j}^{n}}{2}+\frac{k\Delta t}{4\rho C_p(\Delta z)^2}\left[T_{i,j-1}^{n}-2T_{i,j}^{n}+T_{i,j+1}^{n}-T_{i,j-1}^{n+1}\right.\\ &\left.+2T_{i,j}^{n+1}-T_{i,j+1}^{n+1}\right]+\frac{S_j^{n+1/2}-S_j^{n}}{2}.\end{aligned}$$

Knowing that $\frac{S_j^{n+\frac{1}{2}}-S_j^{n}}{2}=0$, and introducing the intermediate function $\tau(t,x,z)$ which resembles to $T_{i,j}^{n+\frac{1}{2}}$:

$$\begin{aligned}&\tau(t,x,z)\\ &=\frac{T(t+\Delta t,x,z)+T(t,x,z)}{2}+\frac{k\Delta t}{4\rho C_p(\Delta z)^2}\left[T(t,x,z-\Delta z)\right.\\ &-2T(t,x,z)+T(t,x,z+\Delta z)-T(t+\Delta t,x,z-\Delta z)+2T(t+\Delta t,x,z)\\ &\left.-T(t+\Delta t,x,z+\Delta z)\right].\end{aligned}$$

For any solution T of the heat equation, the truncation error coming from equation (5.5) is

$$\begin{aligned}(5.10)\qquad &E_{Trun}(T)\\ &=\frac{\tau(t,x,z)-T(t,x,z)}{\Delta t}+\frac{k}{2\rho C_p(\Delta x)^2}\left[-\tau(t,x-\Delta x,z)+2\tau(t,x,z)\right.\end{aligned}$$

$$-\tau(t,x+\Delta x,z)] + \frac{k}{2\rho C_p(\Delta z)^2}\left[-T(t,x,z-\Delta z)\right.$$
$$\left. +2T(t,x,z) - T(t,x,z+\Delta z)\right]$$

where τ is defined by equation (5.10). The Taylor expansion gives

$$\begin{aligned} \tau &= T + \frac{\Delta t}{2}\frac{\partial T}{\partial t} + \frac{(\Delta t)^2}{4}\left(\frac{\partial^2 T}{\partial t^2} - \frac{k}{\rho C_p}\frac{\partial^3 T}{\partial t \partial z^2}\right) \\ &+ \frac{(\Delta t)^3}{24}\left(2\frac{\partial^3 T}{\partial t^3} - 3\frac{k}{\rho C_p}\frac{\partial^4 T}{\partial t^2 \partial z^2}\right) \\ &+ O\left[(\Delta t)^3 + (\Delta t)(\Delta z)^2\right] \end{aligned} \tag{5.11}$$

and hence

$$\begin{aligned} E_{Trun}(T) = \frac{\tau - T}{\Delta t} - \frac{k}{\rho C_p}&\left[(\frac{\partial^2 \tau}{\partial x^2} + \frac{(\Delta x)^2}{12}\frac{\partial^4 \tau}{\partial x^4} + \frac{\partial^2 T}{\partial z^2} + \frac{(\Delta z)^2}{12}\frac{(\partial^4 T}{\partial z^4}\right] \\ + O[(\Delta x)^2 + (\Delta z)^2] \end{aligned} \tag{5.12}$$

Thus

$$\begin{aligned} E_{Trun}(T) &= \left(\frac{k}{\rho C_p}\right)^3 \frac{(\Delta)^2 t}{24}\Delta\left(\frac{\partial^4 T}{\partial x^2 \partial z^2} - \Delta^2 T\right) \\ &- \frac{k}{24\rho C_p}\left[(\Delta x)^2\frac{\partial^4 T}{\partial x^4} + (\Delta z)^2\frac{\partial^4 T}{\partial z^4}\right] \\ &+ O\left[(\Delta x)^2 + (\Delta z)^2 + (\Delta t)^2\right], \end{aligned} \tag{5.13}$$

where Δ (alone) denotes the laplacian operator. Therefore the scheme is consistent of order 2.

b)] Stability Equations (5.3) and (5.4) are rewritten as

$$\left[I + \frac{\Delta t}{2}V_1\right]T^{n+\frac{1}{2}} = \left[I - \frac{\Delta t}{2}V_2]T^n + \frac{\Delta t}{2}V_2\right]S_j^n, \tag{5.14}$$

$$\left[I + \frac{\Delta t}{2}V_2\right]T^{n+1} = \left[I - \frac{\Delta t}{2}V_1\right]T^{n+\frac{1}{2}} + \frac{\Delta t}{2}S_j^{n+\frac{1}{2}}. \tag{5.15}$$

By eliminating $T^{n+\frac{1}{2}}$ from relations (5.10) and (5.10), the system giving T^{n+1} directly as a function of T^n is written as

$$\begin{aligned} T^{n+1} &= (I + \frac{\Delta t}{2}V_2)^{-1}(I - \frac{\Delta t}{2}V_1)(I - \frac{\Delta t}{2}V_1)^{-1}(I - \frac{\Delta t}{2}V_2)T^n \\ &+ (I + \frac{\Delta t}{2}V_2)^{-1}(I - \frac{\Delta t}{2}V_1)(I + \frac{\Delta t}{2}V_1)^{-1}\frac{\Delta t}{2}S_j^n + \frac{\Delta t}{2}S_j^{n+\frac{1}{2}}. \end{aligned} \tag{5.16}$$

Since V and W are commutative matrices, we can write

$$T^{n+1} = W_2 W_1 T^n + W_1 \left(I + \frac{\Delta t}{2}V_2 \right)^{-1} \frac{\Delta t}{2}S_j^n + \frac{\Delta t}{2}S_j^{n+\frac{1}{2}}, \tag{5.17}$$

with

$$W_1 = (I - \frac{\Delta t}{2}V_1)(I + \frac{\Delta t}{2}V_1)^{-1}$$

and

$$W_2 = (I - \frac{\Delta t}{2}V_2)(I + \frac{\Delta t}{2}V_2)^{-1}.$$

Given that V_1 and V_2 are symmetric matrices, and by the use of lemma 3.1 [16], the matrices W_1 and W_2 are symmetric. In addition the matrices V and W are also positive-semi-definite. Hence we have: $||W_1||_2 - \eta(W_1) \leq 1$ and $||W_2||_2 - \eta(W_2) \leq 1$. with $\eta(W) = max|\lambda_k|$ and $|\lambda_k| = \frac{|1-\alpha\mu_k|}{1+\alpha\mu_k} \leq 1$, where μ_k are the eigenvalues of V_1 and V_2 for $\alpha \geq 0$.This confirms the unconditional stability in L^2 norm. Since the ADI numerical scheme is stable and consistent and on the basis of Lax-Richtmyer equivalence theorem [15], it is also convergent.

5.3. **Comparison and validation of results.** In most previous works dealing with solar ponds modeling, the mathematical problem treatment is one-dimensional. In other words, the heat diffusion occurs only along the vertical direction assuming that the temperature of one layer is constant. But, in fact, both horizontal and vertical diffusion are taken into account. The results of numerical simulation have shown that a difference in temperature within the same layer exists and can reach $5°C$ for one season which contradicts the one-dimensional assumption mentioned above and shows the important role played by two-dimensional mathematical modeling. Furthermore, if we compare the present work with respect to the work of Benmansour [17] as well as of Alimi quoted therein which deal with similar problems of solar ponds in two dimensions in regions with similar climatic conditions to those of Annaba (Tunisia is 200 km away from Annaba), we remark, using Figure 8, that there is a similarity between their works (for $\mu = 0.8m - 1$) and ours (for $\mu = 0.5m - 1$) despite this difference in the coefficient μ.

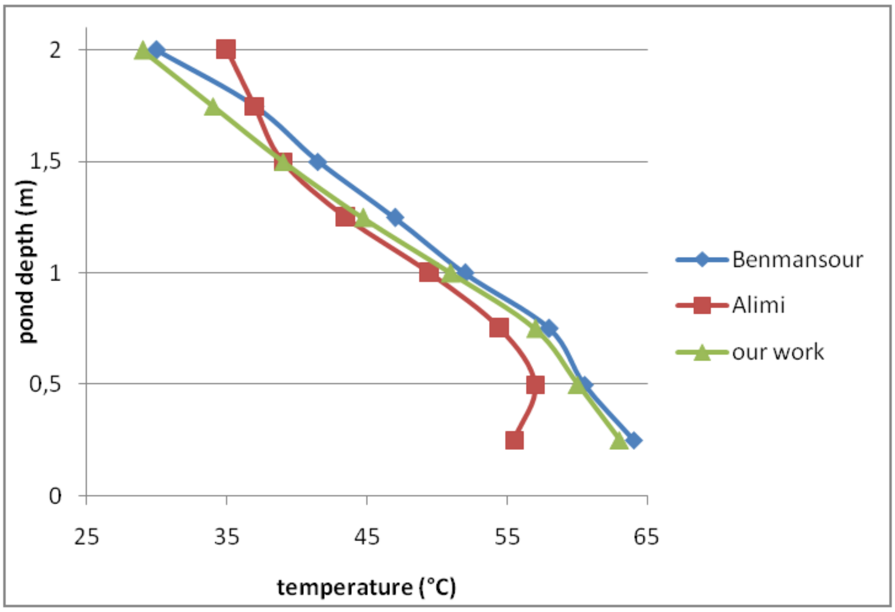

FIGURE 11. Comparison of the present work with previous works

6. CONCLUSION

The behavior of a solar pond represented mathematically by using a transient two-dimensional parabolic model discretized by a numerical scheme based on ADI method due to its good properties of precision and unconditional stability has been used. This simulation was carried out by taking into account the influence of the physical and thermodynamic properties such as thermal conductivity k, the density ρ, specific heat C_p and solar radiation E. The analysis of the numerical results leads to the following conclusions: There is a relatively significant horizontal heat diffusion along the layers which is not observed in the case of one-dimensional studies of ponds. In addition, the temperature reaches a maximum in the central vertical plane of the basin and decreases in the vicinity of the walls. This will give rise to a bigger vertical heat flow at the periphery than at the center. The horizontal profile of the temperature in one-dimensional simulation appears to be flat showing that the temperature is uniform in the horizontal plane of the basin and prevents heat losses through the sides which is far from the reality. The two-dimensional work, on the other hand, presents a convex profile of temperature which highlights the existence of these losses. It can also be noted that temperature values for a given depth become closer with decreasing discretization step, i.e. indicating a trend of convergence towards the exact solution corroborating the theoretical convergence result given above. After 28 days, the obtained results give a maximum estimated temperature in the storage zone of $33°C$ in the winter and a maximum estimated temperature of $66°C$ in the summer. Therefore, it is preferable to fill the pond at the beginning of the summer season to reach quickly the operating temperature of the solar pond where the latter is considered in the present case to be greater than $60°C$. The results obtained in the present work by simulation of heat diffusion equation need to be validated experimentally once the solar pond is operational.

NOMENCLATURE

C_p: Specific heat $[kJ/kg°C]$
E: Radiation intensity $[w/m^2]$
h: Heat Transfer Coefficient $[w/m^{2°}C]$
k: Heat Conductivity Coefficient $[w/m°C]$
q or Q: Heat transfer rate $[w/m^2]$
s: Salinity of the brine $[\%]$
T: Temperature $[°C]$
t: Time [sec]
μ: Extinction Coefficient of Transmission Function $[m-1]$
ρ: Density $[kg/m^3]$.

REFERENCES

[1] S. TUNDEE, P. TERDTOON, P. SAKULCHANGSATJATAI, R. SINGH, A. AKBARZADEH: *Heat extraction from salinity-gradient solar ponds using heat pipe heat exchangers*, Elsevier, Solar Energy, (2010), 1706–1716.
[2] K.R. AGHA: *The thermal characteristics and economic analysis of a solar pond coupled low temperature multi stage desalination plant*, Elsevier, Solar Energy, **83** (2009), 501–510.
[3] J.R. HULL, D.L. BUSHNELL, D.G. SEMPSROTE, A. PENA: *Comparative performance evaluation of fertiliser solar pond under simulated conditions*, Elsevier, Renewable energy, (2003), 455–466.

[4] A.K. SAXENA, S. SUGANDHI, M. HUSAIN: *Significant depth of ground water table for thermal performance of salt gradient solar pond*, Elsevier, Renewable Energy, (2009), 790–793.

[5] M. HUSAIN, P.S. PATIL, S.R. PATIL, S.K. SAMDARSHI: *Thermal behavior of a small salinity-gradient solar pond with wall shading effect*, Elsevier, Solar energy, (2004), 281–290.

[6] R.B. MANSOUR, C.T. NGUYEN, N. GALANIS: *Numerical study of transient heat and mass transfer and stability in a salt-gradient solar pond*, Elsevier,International Journal of Thermal Sciences, (2004), 779–790.

[7] M. MAZIDI, M.H. SHOJAEEFARD, M.S. MAZIDI, H. SHOJAEEFARD: *Two-dimensional modeling of a salt-gradient solar pond with wall shading effect and thermo-physical properties dependent on temperature and concentration*, Springer, Journal of Thermal Science, (2011), 362–370.

[8] R. BOUDHIAF, A.B. MOUSSA, M. BACCAR: *A two-dimensional numerical study of hydrodynamic, heat and mass transfer and stability in a salt gradient solar pond*, Molecular Diversity Preservation International, Energies, (2012), 3986–4007.

[9] R. DARROS-BARBOSA, M.O. BALABAN, A.A. TEIXEIRA: *Transient performance of a two-dimensional salt gradient solar pond—A numerical study*, Wiley Online Library, International journal of energy research, (1996), 713–731.

[10] M. BERKANI, H. SISSAOUI, A. ABDELLI, M. KERMICHE, G. BARKER-READ: *Comparison of three solar ponds with different salts through bi-dimensional modeling*, Solar Energy (2015), 56–68.

[11] M. GIESTAS, H. PINA, A. JOYCE: *The influence of radiation absorption on solar pond stability*, Elsevier, International journal of heat and mass transfer, (1996). 3873–3885

[12] R.H. PERRY, D.W. GREEN, J.O. MALONEY: *Perry's Chemical Engineers' Handbook (ed.)*,Seventh, International edition, (1997).

[13] R.M.M. MATTHEIJ, S.W. RIENSTRA, J.H.M. TEN THIJE BOONKKAMP: *Partial differential equations: modeling, analysis, computation*, SIAM, (2005).

[14] B. MATTHEIJ, H. SISSAOUI, A. ABDELLI, M. KERMICHE, G. BARKER-READ: *The effect of thermodiffusion on the stability of a salinity gradient solar pond*, Elsevier, International journal of heat and mass transfer (2015), 4633–4639.

[15] P. MATTHEIJ, D. LAX, R.D. RICHTMYER: *Survey of the stability of linear finite difference equations*, Wiley Online Library, Communications on pure and applied mathematics (1956), 267–293.

[16] J.F. SCHEID: *méthodes numériques pour la dynamique des fluides*,Institut E. Cartan UMR, Institut E. Cartan UMR (2007) 2011–2012.

[17] R. BEN MANSOUR: *Étude numérique du comportement transitoire d'un étang solaire à gradient de salinité*, National Library of Canada= Bibliothèque nationale du Canada, Ottawa (2005), 267–293.

DEPARTMENT OF MATHEMATIC
UNIVERSITY OF TAMANRASSET
ANNABA,
ALGERIA.
Email address: $abdelli_ammar@yahoo.fr$

DÉPARTEMENT DE GÉNIE DE PROCÉDÉS
UNIVERSITÉ BADJI MOKHTAR, BP 12, ANNABA 23000, ALGERIA.
ANNABA,
ALGERIA.
Email address: hsissaoui@hotmail.com

LABORATOIRE DE RECHERCHE LANOS
UNIVERSITÉ BADJI MOKHTAR, BP 12, ANNABA 23000, ALGERIA.
ANNABA,
ALGERIA.
Email address: $kermiche_mgp@yahoo.fr$

DEPARTMENT OF PREPARATORY CLASS
NATIONAL POLYTECHNIC INSTITUTE OF CONSTANTINE
ALI MENDJELI, CONSTANTINE,
ALGERIA.
Email address: bahi.oussama2@gmail.com